Epigenetic factor clusters regulate single-molecule dynamics in living embryonic stem cells

Roubina Tatavosian, Brian Ma, Kyle Brown, Chao Zhen, Huy Nguyen Duc, Alexa Schwerts, Samantha Kent, Thao Ngoc Huynh, and Xiaojun Ren*
University of Colorado Denver, United States Colorado State University, United States

Abstract:

Cbx2-PRC1 is one of the components of PcG complex that plays a critical role in regulation of developmentally regulated genes. However, the molecular mechanism of targeting Cbx2-PRC1 to chromatin is poorly understood. Here, by combining genetic engineering with live cell single-molecule tracking (SMT), we examined molecular mechanism of targeting and binding of Cbx2 at chromatin in mouse embryonic stem cells. Our results demonstrated that N-terminus of Cbx2 is required for chromatin binding, but not the C-terminus. Deletion of N, and C-terminus affected the binding stabilization of Cbx2 at chromatin. Cbx2 can interact with chromatin independent of histone H3 lysine 27 methylation (H3K27me3), while, the absence of H3K27me3 mark can reduce the residence time of cbx2 at chromatin. Moreover, genetic disruptions of PRC1 complex demonstrated that complex formation may not be required for targeting of Cbx2 to chromatin, however, it influences its residence time at chromatin. We show that Cbx2-PRC1 forms clusters in vitro and in Our results suggest that the multiple domains of Cbx2 may required to facilitate together for targeting and stable binding of Cbx2-PRC1 at chromatin.

Figure 1: Quantification of chromatin-binding fractions by

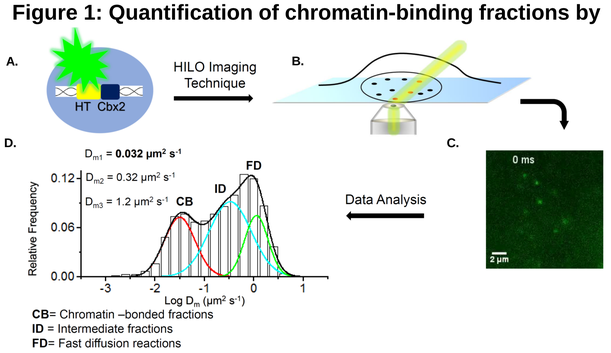

CB= Chromatin –bonded fractions
ID = Intermediate fractions
FD= Fast diffusion reactions

Schematic of experimental approach to quantitively quantify population fractions of Cbx2-PRC1 association with chromatin using single molecule tracking in living mES cells. (**A**) Halotag protein was stably fused at N-terminus of full length Cbx2-PRC1 and varies deletions of Cbx2 proteins. (**B**) Image stacks were acquired by TIRF microscopy with highly inclined thin illumination (HILO) excitation. (**C**) Image of SMT of HT-Cbx2 proteins in the cell nucleus. (**D**) Normalized histogram of the log diffusion maximum likelihood coefficient (D_m) fitted by three component Gaussian distribution function, generating three populations; chromatin bonded (CB, red), intermediate fraction (ID, cyan), and fast diffusion (FD, green) for N-terminus deletion of Cbx2-PRC1 proteins.

Figure 2: Experimental strategy of residence time measurements of Cbx2-PRC1 on chromatin by SMT

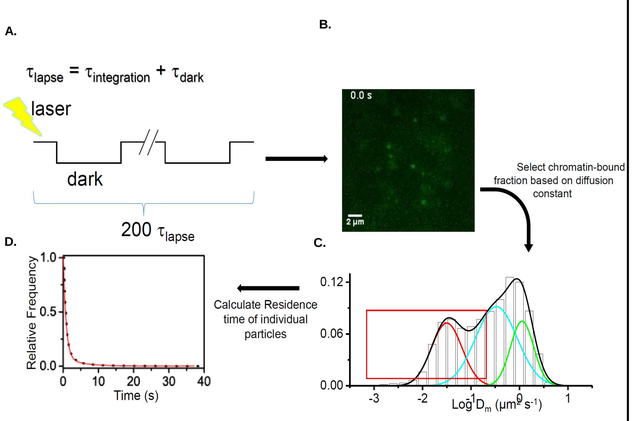

(A) Time-lapse images acquired at an integration time τ_{int}, of 30 ms interspersed with a dark time τ_d, of 170 ms. (**B**) An example of time-lapse image acquired. Each fluorophore spot represents HaloTag-Cbx2 protein in live mES cells. (**C**) Diffusion coefficients of individual HaloTag-Cbx2 molecules calculated and chromatin bonded fraction were selected if their D_m was < 0.10 μm²/s^{-1}. (**D**) The histogram was fitted by a two-component exponential decay function, generating residence time of HaloTag-Cbx2 proteins on chromatin.

Figure 3: The chromatin association of Cbx2 is independent of H3K27me3

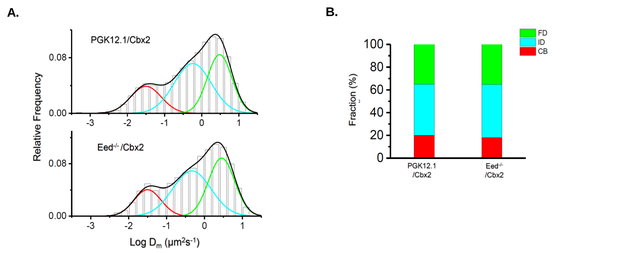

(A) Normalized histogram of the log diffusion coefficient (D_m) for PGK12.1/ HT-Cbx2 (N= 140 cells, n=14484 trajectories), and Eed$^{-/-}$/ Cbx2 (N= 60, n=6317). (**B**) Bar graph of population fractions of (CB, red), (ID, cyan) and (FD, green) for C-terminus deletion of Cbx2-PRC1 proteins.

Figure 4: H3K27me3 is required for residence time of Cbx2 on chromatin

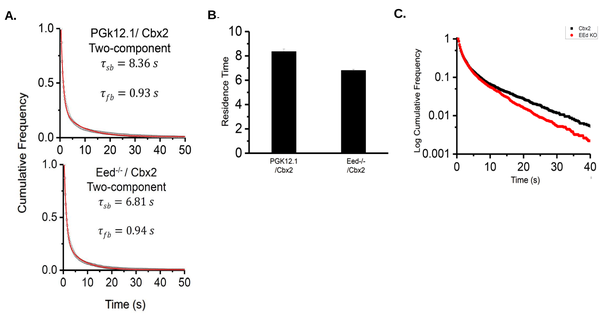

(**A**) Cumulative frequency distribution of the residence time for PGK12.1/Cbx2 (N = 58 cells, n = 5209 trajectories), Eed$^{-/-}$ /Cbx2 (N = 65, n = 6037) in wild-type mES cells. The histograms were fitted with a two-component exponential decay model. (**B**) Bar graph of residence time (τ_{sb}) of the stable chromatin-bound population for PGK12.1/Cbx2 (8.4 s), and Eed$^{-/-}$ /Cbx2 (6.8 s). (**C**) Survival probability graph for PGK12.1/Cbx2, and Eed$^{-/-}$ /Cbx2.

Figure 5: N-Terminus of Cbx2 is required for binding to chromatin

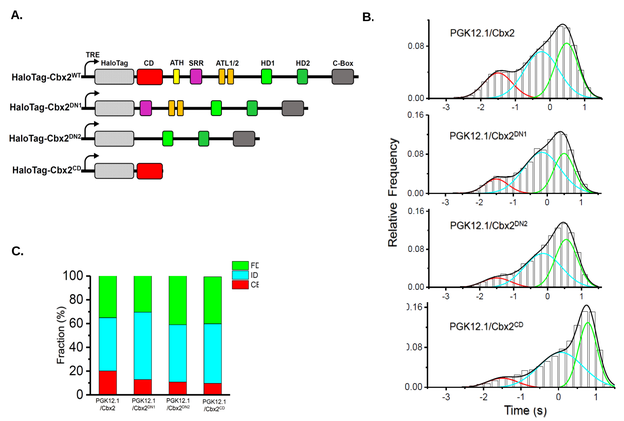

(**A**) Sketch representation of Cbx2-PRC1 N-terminus deletion mutant proteins genetically fused with Halotag were stably expressed in mES wildtype (PGK12.1) cell lines. (**B**) Normalized histogram of the log diffusion coefficient (D_m) for PGK12.1/ HT-Cbx2 (N= 140 cells, n=14484 trajectories), PGK12.1/ Cbx2^{DN1} (N= 5, n=5221), PGK12.1/ Cbx2^{DN2} (N= 86, n=6154), and PGK12.1/ Cbx2^{CD} (N= 149, n=7631. The histograms were fitted with three component Gaussian. (**C**) Bar graph of population fractions of chromatin bonded (CB, red), intermediate fraction (ID, cyan), and fast diffusion (FD, green) for N-terminus deletion of Cbx2-PRC1 proteins.

Figure 6: Residence time of Cbx2 decreases by deletion of N-terminus

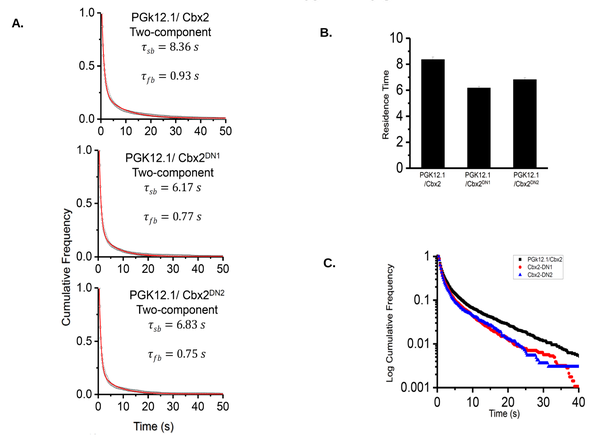

(**A**) Cumulative frequency distribution of the residence time for PGK12.1/Cbx2 (N = 58 cells, n = 5209 trajectories), PGK12.1/Cbx2^{DN1} (N = 116, n = 6433), and PGK12.1/Cbx2^{DN2} (N = 64, n = 2642) in wild-type mES cells. The histograms were fitted with a two-component exponential decay model. (**B**) Bar graph of residence time (τ_{sb}) of PGK12.1/Cbx2 (8.4 s), PGK12.1/ Cbx2^{DN1} (6.2 s) , and PGK12.1/ Cbx2^{DN2} (6.8 s). (**C**) Survival probability graph for PGK12.1/Cbx2, PGK12.1/Cbx2^{DN1}, and PGK12.1/Cbx2^{DN2}.

Figure 7: C-terminus of Cbx2 is not required for binding to chromatin

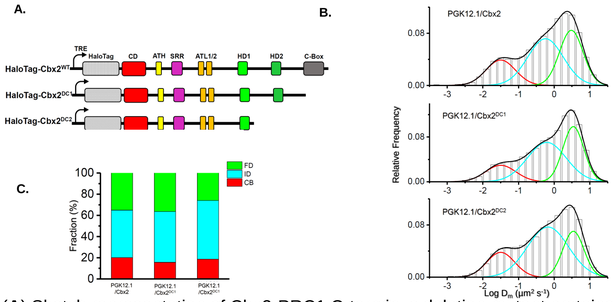

(**A**) Sketch representation of Cbx2-PRC1 C-terminus deletion mutant proteins genetically fused with Halotag were stably expressed in mES wildtype (PGK12.1) cell lines. (**B**) Normalized histogram of the log diffusion coefficient (D_m) for PGK12.1/ Cbx2 (N= 140 cells, n=14484 trajectories), PGK12.1/ Cbx2^{DC1} (N= 75, n=9082), PGK12.1/ Cbx2^{DC2} (N= 64, n=12389), and PGK12.1/ Cbx2^{DC3} (N= 69, n=6124. (**C**) Bar graph of population fractions of (CB, red), (ID, cyan) and (FD, green) for C-terminus deletion of PRC1-Cbx2 proteins.

Figure 8: C-terminus is needed for stabilization of Cbx2 on chromatin

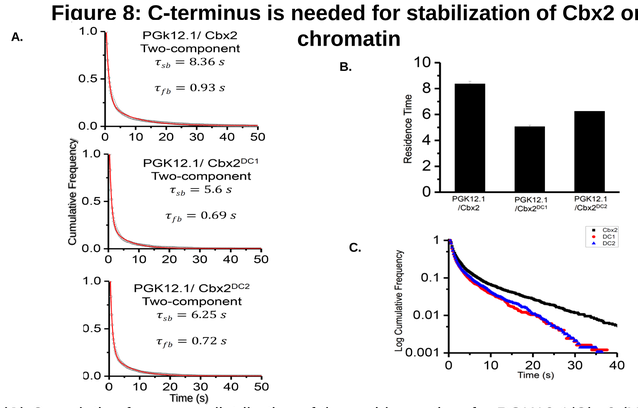

(**A**) Cumulative frequency distribution of the residence time for PGK12.1/Cbx2 (N = 58 cells, n = 5209 trajectories), PGK12.1/Cbx2^{DC1} (N = 103, n = 6513), and PGK12.1/ Cbx2^{DC2} (N = 93, n = 7032), and PGK12.1/Cbx2^{DC3} (N = 124, n = 10958) in wild-type mES cells. The histograms were fitted with a two-component exponential decay model. (**B**) Bar graph of residence time (τ_{sb}) of PGK12.1/Cbx2 (8.4 s), PGK12.1/ Cbx2^{DC1}(5.6 s), PGK12.1/Cbx2^{DC2} (6.3 s),and PGK12.1/Cbx2^{DC3} (7.7 s). (**C**) Survival probability graph for PGK12.1/Cbx2, PGK12.1/Cbx2^{DN1}, and PGK12.1/Cbx2^{DN2}.

Figure 9: PRC1 Complex formation is not be required for targeting of Cbx2 to chromatin

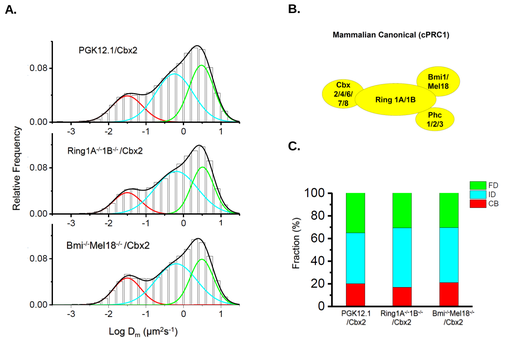

(A) Normalized diagrams of the log diffusion coefficient (D_m) for PGK12.1/ HT-Cbx2 (N= 140 cells, n=14484 trajectories), Ring1A$^{-/-}$ 1B$^{-/-}$ / Cbx2 (N= 66, n=11754), and Bmi$^{-/-}$Mel18$^{-/-}$/ Cbx2 (N= 76, n=9662). (**B**) Sketch of mammalian canonical PRC1. (**C**) Bar graph of population fractions of (CB, red), (ID, cyan) and (FD, green) for C-terminus deletion of Cbx2-PRC1.

Figure 10: Disruption of complex formation effects residence time of Cbx2

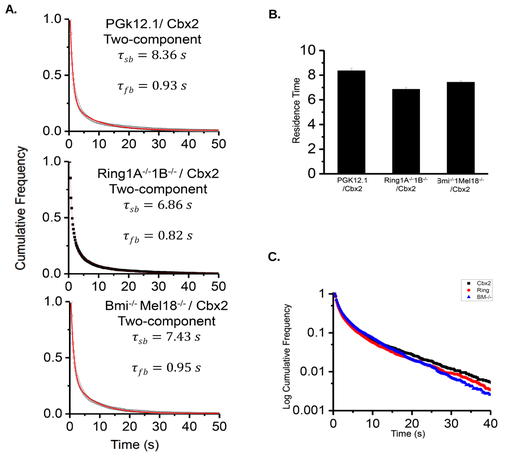

(**A**) Cumulative frequency distribution of the residence time for PGK12.1/Cbx2 (N = 58 cells, n = 5209 trajectories), Ring1A$^{-/-}$ 1B$^{-/-}$ /Cbx2 (N = 59, n = 7070), and Bmi$^{-/-}$ Mel18$^{-/-}$ /Cbx2 (N = 66, n = 7548) in wild-type mES cells. The histograms were fitted with a two-component exponential decay model. (**B**) Bar graph of residence time (τ_{sb}) of the stable chromatin-bound population for PGK12.1/Cbx2 (8.4 s), and Eed$^{-/-}$ /Cbx2 (6.9 s). (**C**) Survival probability graph for PGK12.1/Cbx2, Ring1A$^{-/-}$ 1B$^{-/-}$ /Cbx2 (6.9), and Bmi$^{-/-}$ Mel18$^{-/-}$ /Cbx2 (7.4 s).

Figure 11: Cbx2 forms clusters *in vitro* and *in vivo*

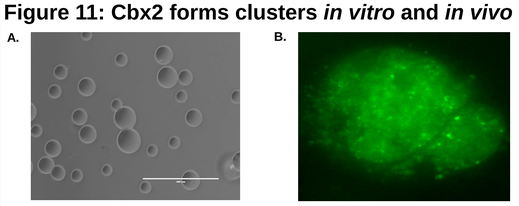

(A) Cbx2 protein forms clusters *in vitro* at 4ºC. **(B)** Live cell image of HeLa cells expressing YFP-Cbx2 (scale 5 μm).

Acknowledgment:
This work was supported, in whole or in part, by the National Cancer Institute of the National Institutes of Health under Award Number R03CA191443 (X.R.). We thank members of Dr. Xiaojun Ren laboratory for their help and support throughout this project.